

Universal Approach to Critical Percolation

Fabian Coupette^{1,*} and Tanja Schilling^{1,†}

¹*Institute of Physics, University of Freiburg, Hermann-Herder-Straße 3, 79104 Freiburg, Germany*

(Dated: September 1, 2023)

Percolation problems appear in a large variety of different contexts ranging from the design of composite materials to vaccination strategies on community networks. The key observable for many applications is the percolation threshold. Unlike the universal critical exponents, the percolation threshold depends explicitly on the specific system properties. As a consequence, theoretical approaches to the percolation threshold are rare and generally tailored to the specific application.

Yet, any percolating cluster forms a discrete network the emergence of which can be cast as a graph problem and analyzed using branching processes. We propose a general mapping of any kind of percolation problem onto a branching process which provides rigorous lower bounds of the percolation threshold. These bounds progressively tighten as we incorporate more information into the theory. We showcase our approach for different continuum problems finding accurate predictions with almost no effort. Our approach is based on first principles and does not require fitting parameters. As such it offers an important theoretical reference in a field that is dominated by simulation studies and heuristic fit functions.

Percolation describes the formation of giant components in complex systems [1, 2]. Originally proposed to describe water permeating a rock through the emergence of a system spanning cavity network [3–6], percolation theory has been applied in a broad variety of different contexts [7, 8] such as the design of composite materials [9–19], the analysis of complex networks [20–24], and transport through porous media [25–29]. The phenomenon attracted particular attention due to its resemblance of a thermodynamic phase transition [30–34], where the percolation probability acts as an order parameter and the mean cluster size can be interpreted as a susceptibility with characteristic power-law exponents describing their scaling behavior in the vicinity of the critical point, i.e., the percolation threshold. While those critical exponents coincide for all standard percolation problems set in the same spatial dimension [35–40], the percolation threshold itself sensitively depends on the intricacies of the system. As a consequence, theoretical approaches are mostly tailored to specific applications [11, 15, 41–47] and straightforward simulation is the primary tool of choice for the accurate determination of critical parameters [33, 48–54]. Yet, the predictive power of these approaches is limited.

Connectivity percolation has been studied with a multitude of different prefixes such as lattice, continuum, directed, dynamic, protected, explosive or bootstrap [8, 55]. In spite of this variety of flavors, percolation inherently is always a graph problem. Even if particles move continuously in space, the connectivity relationship between the particles in the system can be expressed as a graph with each vertex representing a particle and edges corresponding to a connection between the particles represented by the incident vertices.

Thus, each configuration γ of the system translates into a network which we may independently analyze for the existence of a giant component. Therefore, all percolation problems have a unified foundation which we will exploit in the following.

For illustrative purposes consider an infinite connected graph G . Assigning an arbitrary vertex of the graph as the origin, \mathcal{O} , we define the k -neighborhood \mathcal{N}_k of \mathcal{O} as the sub-graph spanned by all random walks of length k starting at the origin. The shortest distance to the origin partitions the vertex set of the complete network into mutually disjoint vertex sets $V_k = V(\mathcal{N}_k) \setminus V(\mathcal{N}_{k-1})$ where $V(\cdot)$ refers to the vertex set of the graph in brackets (cf. Fig. 1). We now define a percolation problem on G by assigning a degree of freedom to each edge, i.e., each edge is either open or closed. Two vertices are considered connected if there is a path of open edges linking them. We call a vertex open if it is connected to the origin. The percolation probability Θ is defined as the probability that the origin is part of an infinite cluster of connected vertices. If the model is taking parameters $\mathbf{p} \in \Lambda$ from a parameter space Λ then the critical manifold (the “percolation threshold”) is defined as the boundary of the set

$$\{\mathbf{p} \in \Lambda : \Theta(\mathbf{p}) = 0\}. \quad (1)$$

Given a configuration of the system, define X_k as the number of open vertices in V_k on the sub-graph \mathcal{N}_k . Accordingly, X_1 is the number of direct neighbors of the origin, i.e., vertices connected to the origin through a single open edge. Direct neighbors of any of these X_1 vertices that have not been visited before comprise X_2 . Continuing in this manner gives rise to a sequence $(X_k)_{k \in \mathbb{N}}$ that we call surface activity sequence. Only the open vertices in V_k have the capacity to induce open vertices in V_{k+1} on \mathcal{N}_k . Consequently, the sequence terminates once $X_k = 0$, i.e. there is a finite cluster around the origin. Notice that through the exclusion of previously visited vertices in the

* fabian.coupette@physik.uni-freiburg.de

† tanja.schilling@physik.uni-freiburg.de

exploration of neighborhoods the graph generated by the modified search algorithm is treelike. Thus, we can interpret the stochastic process as a branching process of the form

$$X_{k+1} = \sum_{i=1}^{X_k} \xi_i^k \quad \text{with} \quad X_0 = 1, \quad (2)$$

with ξ_i^k being a random variable describing the distribution of next-level neighbors generated by the i^{th} member of the k -neighborhood. The extinction probability Q of this branching process is $Q = 1 - \Theta$. At this stage it is irrelevant whether the sequence $(X_k)_{k \in \mathbb{N}}$ was generated by bond percolation on the square lattice, cavities in a porous medium, or carbon nano-tubes dispersed in a polymer matrix. We can carry out this mapping for any percolation problem, but naturally we only transfer the original complexity onto the definition of the random variables ξ_i^k . So what is all this good for?

There are two different aspects contributing to the complexity of ξ_i^k on the graph level: vertex correlations and loop structure. The former can express itself as, for instance, the friendship paradox [56, 57] in social networks or the structure of a hard sphere fluid [58]. These correlations can be both, positive as well as negative, and they tend to decay with the distance between layers of the construction. In simplified terms, vertex correlations account for the k -dependence of ξ_i^k . Loops, on the other hand, exclusively induce negative correlations. The redundancy of multiple paths activating the same surface vertex leads to a reduced average surface activity compared to counting each path individually [4]. We are going to exploit this one-sided correlation in the following when constructing a lower bound for the percolation threshold.

Treelike networks are an important special case as they allow for exact calculation of the percolation threshold [59]. Without loops, the probability distributions corresponding to the individual ξ_i^k only depend on the distribution of vertex degrees across the system. If, furthermore, the network is asymptotically homogeneous, i.e., $\xi^k \rightsquigarrow \xi$ converges in distribution to a common random variable ξ (sometimes involving a coarse-graining step cf. Fig. 1), the problem simplifies to a Galton-Watson branching process [60]. As a consequence, the percolation problem on a treelike network is critical if

$$\mathbb{E}[\xi] = 1, \quad (3)$$

i.e., an active vertex induces on average another active vertex on the next level. The random variable ξ captures the recurring transition from one layer of the construction to the next. If the network features degree correlations (cf. right panel of Fig. 1) the definition of ξ may require an additional coarse-graining step but the criticality condition remains valid. As these degree correlations do not fundamentally change the problem we will ignore them for the moment. Loops are the actual problem.

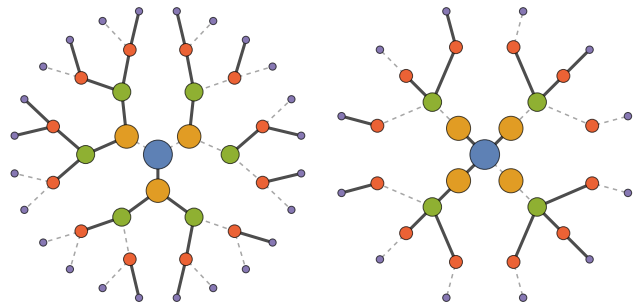


Figure 1. Impact of vertex correlations: fragments of two treelike lattices with the same mean vertex degree $\langle z \rangle = 3$. Left: Globally homogeneous vertex degree, i.e., regular Bethe lattice, with critical edge probability $p_c = \frac{1}{\langle z \rangle - 1} = \frac{1}{2}$. Right: Vertex degree alternates between 2 and 4 on every path across the lattice. Coarse-graining two subsequent branching steps into one we recover a homogeneous Bethe lattice with $p_c = \frac{1}{\frac{1}{\sqrt{3}} + 1} > \frac{1}{2}$. Colors and vertex sizes distinguish the vertex sets V_k . Edges illustrate a realization of a bond percolation model: thick bonds are open, dashed bonds are closed.

When casting percolation on a network with cycles on a branching process we effectively replace loops by correlations between the random variables ξ^i that control the propagation of the surface activity. The distribution of X_{k+1} is not entirely defined by X_k but also depends on the position of the active surface vertices relative to each other.

If the length of loops is bounded throughout the system, we can coarse-grain to absorb the largest loop in a single branching step and solve the network as a decorated Bethe lattice. Indeed, the significance of loops of diverging size constitutes the universality class of the percolation problem. However, a loop comprises two independent paths leading to the same surface vertex. If we add the probability of each path to be open, we systematically overestimate the average surface activity by neglecting loops. For systems containing only loops of finite length we can apply our previous solution strategy, integrate out the largest loops and use eq. (3) to compute the percolation threshold. That means, without vertex correlations,

$$\mathbb{E}[X_k] = 1, \quad (4)$$

always provides a lower bound to the percolation threshold which becomes progressively more precise as k is increased. Eq. (4) gives rise to a hierarchy of approximations. We call this hierarchy *areal expansion* in analogy to the virial expansion, because in the continuum we will systematically integrate out larger volumes rather than expanding in the number of particles participating in an interaction.

For $k = 1$, eq. 4 assumes an entirely treelike network topology which is equivalent to the second virial approximation and thus consistent with the exactly solved percolation models [59]. For $k = 2$, we correctly

incorporate loops comprising up to four edges. As k goes to infinity we eventually integrate out the entire system and the lower bound necessarily becomes arbitrarily tight. Naturally, we cannot compute X_k analytically for large k in complicated systems so that, regarding the exact value of the percolation threshold, we do not gain anything compared to a straightforward simulation. The strength of our approach is that we can compute reliable lower bounds with decent precision with little effort. Moreover, analytical results for low orders of the construction enable us to directly characterize the impact of model parameters on the percolation threshold.

To demonstrate the virtues of our approach, consider one of the most fundamental continuum percolation problems: points randomly distributed in \mathbb{R}^3 with a prescribed number density ρ . Points are connected if their separation is smaller than a parameter d . Above a critical dimensionless density $\rho_c d^3 \approx 0.6530$ [50], the system almost surely contains an infinite cluster of connected points. While established simulation techniques allow for an accurate determination of this value, theoretical approaches like connectedness percolation theory employing liquid state theory for connectivity are generally inconclusive. The virial series cannot be truncated at any accessible order [61, 62] and liquid state closures to the connectedness Ornstein-Zernike equation generate wrong diagrammatic expansions [41, 43, 63–65]. Other methods which provide accurate predictions are either heuristic in nature, based on unjustifiable assumptions or tailored to specific systems [17, 66, 67]. With all these approaches, it is extremely hard to *a priori* estimate the accuracy of the result which renders their predictive power virtually inexistent.

The areal approximation has a straightforward continuum formulation. We decompose the probability $p(\mathbf{r}_1, \mathbf{r}_2)$ that particles positioned at \mathbf{r}_1 and \mathbf{r}_2 are connected into functions p_k , which describe the connection probability with the additional constraint that the shortest path between them has length k

$$p(\mathbf{r}_1, \mathbf{r}_2) = \sum_{k=1}^{\infty} p_k(\mathbf{r}_1, \mathbf{r}_2). \quad (5)$$

$p_k(\mathcal{O}, \mathbf{r})$ describes the probability density that a particle at \mathbf{r} is activated in the k^{th} branching step. Accordingly, the average number of particles activated in the k^{th} branching step, i.e., X_k , is given by

$$\mathbb{E}[X_k] = \int d\mathbf{r} \rho(\mathbf{r}) p_k(\mathcal{O}, \mathbf{r}). \quad (6)$$

Combining eq. (4) and eq. (6), we find a sequence $(\rho_c^k)_{k \in \mathbb{N}}$ of rigorous lower bounds for the percolation threshold of a continuum percolation problem. However, the graph distance is not the natural length scale for a continuum system. Thus, we are going to improve the approach with two slight modifications.

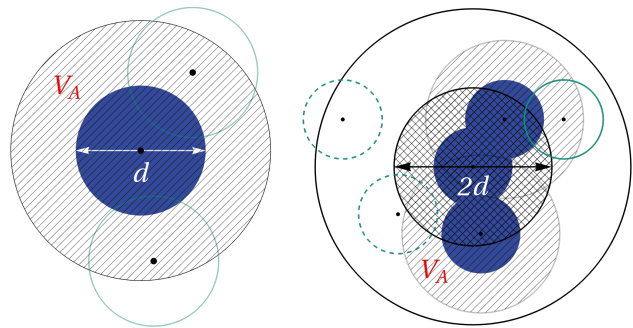


Figure 2. Penetrable disks of diameter d . Left: Areal order $k = 1$. The blue particle in the origin is isolated unless there is at least one particle centered in the active volume V_A (hatched). The average number of particles within this area becomes $\mathbb{E}[X_1]$. Right: Areal order $k = 2$. We fix a configuration within the central disk of radius of $(k - 1)d$. The corresponding cluster nucleus remains finite unless there is at least one particle in the new active volume V_A (hatched). The crossed area is already specified so that it does not contribute to V_A . Averaging ρV_A over all configurations in the crossed area (origin fixed) gives us $\mathbb{E}[X_2]$.

Eq. (6) effectively approximates the cluster containing the origin as a tree of k -neighborhoods. We can switch to euclidean distance by adapting our notion of a k -neighborhood: instead of referring to the particles that can be reached by a random walk of k -steps from the origin on the connectivity graph, we include all particles that can be reached by a random walk that does not exit the ball $\mathcal{B}_k(\mathcal{O})$ of radius k (euclidean distance) around the origin. The cluster containing the origin is almost surely finite if there is not on average at least one particle outside of the ball connected to the k -neighborhood. Now we define $\mathbb{E}[X_{k+1}]$ as the average number of particles in direct contact with the k -neighborhood outside of the k -ball averaged over all system configurations.

Applying our approach to the sphere model (and generally to all non-interacting models) is particularly simple: Due to a homogeneous density distribution,

$$\mathbb{E}[X_{k+1}] = \rho \mathbb{E}[V_A(k)], \quad (7)$$

with the active volume $V_A(k) \subset \mathcal{B}_k(\mathcal{O})^c$ of a configuration defined as the volume outside of the k -ball in which a probe particle would intersect the k -neighborhood of the origin (see Fig. 2). The active volume comprises the set of positions which have the capacity to further extend the cluster that contains the origin. For spheres, $V_A(0)$ is simply the excluded volume of the origin. This is equivalent to the second virial approximation as required for consistency with exactly solvable models. Yet, the third virial order accounts only for the addition of triangles which does not yield a real percolation threshold (see [62]). Conversely, the second areal approximation contains all configurations of the ball $\mathcal{B}_d(\mathcal{O})^c$, e.g., complete graphs to arbitrary order. Moreover, the areal

Table I. Lower bounds for the percolation threshold calculated with areal and virial approximation.

order k	areal $\rho_c^{kd} d^3$	ar. half-space $\tilde{\rho}_c^{kd} d^3$	virial
1	0.2387	0.4775	—
2	0.3468	0.5502	0.2387
3	0.4375	0.5959	—
4	0.4874	0.6099	0.3001
Simulation	0.6530	0.6530	0.6530

approximation by design provides lower bounds of the percolation thresholds which tighten as we increase the order of the expansion. The results for the first orders are summarized in Tab. I – the first two areal orders are calculated analytically, for the rest we use small scale Monte Carlo integration.

However, despite a substantial improvement over the virial approximation, the lower bounds are still not particularly tight. This is because we have ignored vertex correlations. Here, our second improvement comes in. The origin has a full 4π solid angle available to branch to, whereas a particle on the surface of the growing cluster after j branching iterations can only grow outward as we already integrated out a ball of radius $(j-1)d$. If j is large but finite we still find for any $\rho > 0$ an open particle J on the surface of the cluster with finite probability. Thus, the system percolates if a branching process initiated at J does not eventually terminate with probability 1. Yet, if j is sufficiently large, the branching process starting at J is effectively constrained to a half-space. By switching from the origin to J , we remove the vertex degree correlations caused by the artificial symmetry of the origin, getting rid of the explicit k -dependence ξ_i^k in eq. (2) by “fast-forwarding to infinity”. Fig. 3 depicts the average surface activity for the constrained branching process. The resultant lower bounds to the percolation threshold $\tilde{\rho}_c^{kd}$ have significantly tightened (see Tab. I). Moreover, the mean surface activities for different orders k mutually intersect each other in close proximity, at a density likewise close to the literature critical density. This pattern is familiar from finite size scaling analysis and exact for treelike networks (see e.g. ref. [59]). For general systems we expect the intersection point to drift slightly towards the percolation threshold.

Finally, we use our method to study the impact of particle anisotropy on the percolation threshold. Consider a penetrable spherocylinder of thickness d and length $l+d$, l being the length of the linear segment, and define its aspect ratio $\zeta := 1 + \frac{l}{d}$. In the Onsager limit $\zeta \rightarrow \infty$, the second virial approximation becomes exact [11], but for $\zeta < 100$ the approximation is inaccurate as simulation studies have shown [53, 68, 69]. Heuristic corrections have been proposed by subjecting the critical number of nearest-neighbors to a power-law fit in the aspect ratio

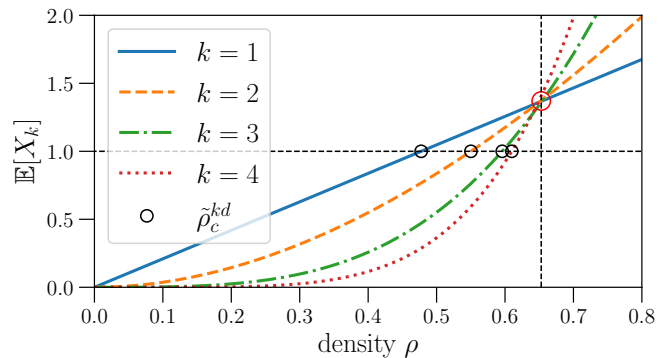


Figure 3. Mean surface activity $\mathbb{E}[X_k]$ of fully penetrable spheres as a branching process constrained to a half-space. For $k \leq 2$ the $\mathbb{E}[X_k]$ can be computed analytically, for $k > 2$ we use small-scale simulations. The circles mark the roots of $\mathbb{E}[X_k] = 1$ corresponding to the lower bounds listed in Tab. I. The red circle contains all mutual intersections between the surface activities at different orders. The vertical dashed line demarcates the critical density determined with high-precision simulations [50].

[68, 69]. But the functional form of this fit is unjustified and does not agree with later simulation studies [53]. We can improve on the second virial approximation using the areal framework: we integrate out a ball of radius ζ and average the number of next-nearest neighbors. We place the center of the first spherocylinder at the origin with a random orientation, fill the ζ -ball with a fixed number of randomly placed and randomly oriented cylinders, and average the active volume of the resulting arrangement over many different configurations. Convolving the result with a Poisson distribution with mean ρV_ζ , where V_ζ is the volume of the specified ζ -ball, yields $\mathbb{E}[X_2]$ as a function of the density. The solutions to $\mathbb{E}[X_2] = 1$ for different aspect ratios lead to the lower bounds ρ_c^2 illustrated in Fig. 4. We observe only a slight improvement over the second virial approximation (ρ_c^1). But, once more, we can constrict the branching process to a half-space to find a massive tightening of the lower bound. The relative deviation to the simulation results is most pronounced for $\zeta = 2$ ($\lesssim 20\%$) and decreases monotonically with ζ ($\approx 10\%$ at $\zeta = 21$). This is expected as the importance of loops in the formation of the percolating cluster diminishes with the aspect ratio ultimately approaching treelike topology in the Onsager limit. It should be emphasized that we find this accuracy for the lowest order above the second virial approximation – the sampling simulation requires at most a few tens of cylinders. This demonstrates that the severe shortcoming of the second virial approximation is not primarily the neglect of loops but rather the omission of vertex degree correlations. In summary, we introduced a general mapping of percolation problems onto branching processes. It is easily applicable to any type of percolation problem: pick an origin and define a notion of k -neighborhood, construct the corresponding random variables X_k and solve

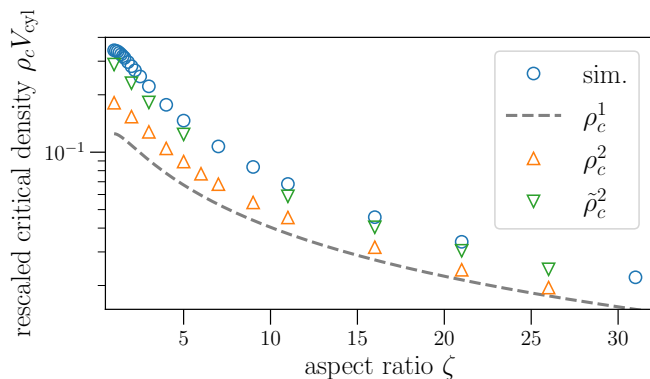


Figure 4. Percolation thresholds for penetrable cylinders with different aspect ratios ζ . V_{cyl} is the volume of the corresponding (sphero)-cylinder. The simulation results (blue circles) are taken from [53]. The dashed line corresponds to the second virial approximation. The different areal approximants are calculated for linear chains of densely overlapping spheres – V_{cyl} is modified accordingly.

$\mathbb{E}[X_k] = 1$ to obtain rigorous lower bounds to the percolation threshold. If the origin is not representative for the asymptotic cluster growth, be it through additional symmetry, an external field or vertex correlations on a lattice, modify X_k to reflect the asymptotic branching process. The resulting lower bounds to the percolation threshold include the first k virial orders and extrapolate, in contrast to the Padé approximation, in a meaningful physical way. Through consistency with the virial approximation we obtain the correct response of critical parameters to small parameter changes in combination with quantitatively accurate predictions.

ACKNOWLEDGMENTS

We acknowledge funding by the German Research Foundation in the project 457534544. Moreover, we thank Christoph Widder for constructive comments and helpful feedback on the manuscript.

-
- [1] D. Stauffer and A. Aharony, *Introduction to percolation theory* (CRC press, 1991).
- [2] G. Grimmett, *Percolation* (Springer, 1999).
- [3] S. R. Broadbent and J. M. Hammersley, in *Mathematical proceedings of the Cambridge philosophical society*, Vol. 53 (Cambridge University Press, 1957) pp. 629–641.
- [4] J. M. Hammersley, *The Annals of Mathematical Statistics* **28**, 790 (1957).
- [5] M. F. Sykes and J. W. Essam, *Journal of Mathematical Physics* **5**, 1117 (1964).
- [6] S. Kirkpatrick, *Reviews of modern physics* **45**, 574 (1973).
- [7] M. Sahimi, *Applications of percolation theory* (CRC Press, 1994).
- [8] A. A. Saberi, *Physics Reports* **578**, 1 (2015).
- [9] L. Flandin, T. Prasse, R. Schueler, K. Schulte, W. Bauhofer, and J.-Y. Cavaille, *Physical Review B* **59**, 14349 (1999).
- [10] J. Sandler, J. Kirk, I. Kinloch, M. Shaffer, and A. Windle, *Polymer* **44**, 5893 (2003).
- [11] A. V. Kyrylyuk and P. van der Schoot, *Proceedings of the National Academy of Sciences* **105**, 8221 (2008).
- [12] W. Bauhofer and J. Z. Kovacs, *Composites science and technology* **69**, 1486 (2009).
- [13] R. H. Otten and P. van der Schoot, *Physical review letters* **103**, 225704 (2009).
- [14] C.-W. Nan, Y. Shen, and J. Ma, *Annual Review of Materials Research* **40**, 131 (2010).
- [15] A. P. Chatterjee, *The Journal of chemical physics* **132** (2010).
- [16] B. Nigro, C. Grimaldi, P. Ryser, A. P. Chatterjee, and P. Van Der Schoot, *Physical review letters* **110**, 015701 (2013).
- [17] F. Coupette, R. de Bruijn, P. Bult, S. Finner, M. A. Miller, P. van der Schoot, and T. Schilling, *Physical Review E* **103**, 042115 (2021).
- [18] F. Coupette, L. Zhang, B. Kuttich, A. Chumakov, S. V. Roth, L. González-García, T. Kraus, and T. Schilling, *The Journal of Chemical Physics* **155** (2021).
- [19] A. P. Chatterjee and C. Grimaldi, *Journal of statistical physics* **188**, 29 (2022).
- [20] C. Moore and M. E. Newman, *Physical Review E* **61**, 5678 (2000).
- [21] G. T. Cantwell and M. E. Newman, *Proceedings of the National Academy of Sciences* **116**, 23398 (2019).
- [22] A. Allard and L. Hébert-Dufresne, *Physical Review X* **9**, 011023 (2019).
- [23] M. Li, R.-R. Liu, L. Lü, M.-B. Hu, S. Xu, and Y.-C. Zhang, *Physics Reports* **907**, 1 (2021).
- [24] M. Newman, *Proceedings of the Royal Society A* **479**, 20220774 (2023).
- [25] W. Rossen and P. Gauglitz, *AICChE Journal* **36**, 1176 (1990).
- [26] B. Berkowitz and I. Balberg, *Water Resources Research* **29**, 775 (1993).
- [27] S. Torquato, *Random heterogeneous materials: microstructure and macroscopic properties* (Springer, 2002).
- [28] A. Hunt, R. Ewing, and B. Ghanbarian, *Percolation theory for flow in porous media*, Vol. 880 (Springer, 2014).
- [29] A. G. Hunt and M. Sahimi, *Reviews of Geophysics* **55**, 993 (2017).
- [30] A. Coniglio, *Physical Review Letters* **46**, 250 (1981).
- [31] M. Aizenman and D. J. Barsky, *Communications in Mathematical Physics* **108**, 489 (1987).
- [32] H.-O. Georgii and O. Häggström, *Communications in mathematical physics* **181**, 507 (1996).
- [33] J. L. Jacobsen, *Journal of Physics A: Mathematical and Theoretical* **47**, 135001 (2014).
- [34] H. Duminil-Copin, A. Raoufi, and V. Tassion, *Annals of Mathematics* **189**, 75 (2019).
- [35] D. Stauffer, *Physics reports* **54**, 1 (1979).
- [36] J. W. Essam, *Reports on progress in physics* **43**, 833 (1980).
- [37] T. Vicsek and J. Kertesz, *Journal of Physics A: Mathematical and General* **14**, L31 (1981).

- [38] S. B. Lee and S. Torquato, *Physical Review A* **41**, 5338 (1990).
- [39] S. Smirnov and W. Werner, *Mathematical Research Letters* **8**, 729 (2001).
- [40] J. A. Gracey, *Physical Review D* **92**, 025012 (2015).
- [41] A. Coniglio, U. De Angelis, and A. Forlani, *Journal of Physics A: Mathematical and General* **10** (1977).
- [42] H. Kesten *et al.*, *Communications in mathematical physics* **74**, 41 (1980).
- [43] T. DeSimone, S. Demoulini, and R. M. Stratt, *The Journal of chemical physics* **85** (1986).
- [44] J. Cardy and R. M. Ziff, *Journal of statistical physics* **110**, 1 (2003).
- [45] F. Wu, *Physical Review E* **81**, 061110 (2010).
- [46] B. Karrer and M. E. Newman, *Physical Review E* **82**, 016101 (2010).
- [47] C. Widder and T. Schilling, *Physical Review E* **104**, 054305 (2021).
- [48] M. D. Rintoul and S. Torquato, *Journal of physics a: mathematical and general* **30**, L585 (1997).
- [49] C. D. Lorenz and R. M. Ziff, *Physical Review E* **57**, 230 (1998).
- [50] C. D. Lorenz and R. M. Ziff, *The Journal of Chemical Physics* **114**, 3659 (2001).
- [51] M. A. Miller and D. Frenkel, *Physical review letters* **90**, 135702 (2003).
- [52] S. Mertens and C. Moore, *Physical Review E* **86**, 061109 (2012).
- [53] T. Schilling, M. A. Miller, and P. Van der Schoot, *Europhysics Letters* **111**, 56004 (2015).
- [54] W. Xu, J. Wang, H. Hu, and Y. Deng, *Physical Review E* **103**, 022127 (2021).
- [55] N. Araújo, P. Grassberger, B. Kahng, K. Schrenk, and R. M. Ziff, *The European Physical Journal Special Topics* **223**, 2307 (2014).
- [56] Y.-H. Eom and H.-H. Jo, *Scientific reports* **4**, 1 (2014).
- [57] G. T. Cantwell, A. Kirkley, and M. Newman, *Journal of Complex Networks* **9**, cnab011 (2021).
- [58] J.-P. Hansen and I. R. McDonald, *Theory of simple liquids* (Elsevier, 1990).
- [59] F. Coupette and T. Schilling, *Physical Review E* **105**, 044108 (2022).
- [60] T. E. Harris *et al.*, *The theory of branching processes*, Vol. 6 (Springer Berlin, 1963).
- [61] U. Alon, A. Drory, and I. Balberg, *Physical Review A* **42**, 4634 (1990).
- [62] Details can be found in the Supplemental Material which includes reference [70].
- [63] Y. Chiew and E. Glandt, *Journal of Physics A: Mathematical and General* **16**, 2599 (1983).
- [64] Y. C. Chiew and G. Stell, *The Journal of chemical physics* **90**, 4956 (1989).
- [65] F. Coupette, *Percolation: Connecting the Dots*, Ph.D. thesis, University of Freiburg (2023), <https://doi.org/10.6094/UNIFR/236560>.
- [66] U. Alon, I. Balberg, and A. Drory, *Physical review letters* **66**, 2879 (1991).
- [67] E. Garboczi, K. Snyder, J. Douglas, and M. Thorpe, *Physical review E* **52**, 819 (1995).
- [68] L. Berhan and A. Sastry, *Physical Review E* **75**, 041120 (2007).
- [69] R. M. Mutiso, M. C. Sherrott, J. Li, and K. I. Winey, *Physical Review B* **86**, 214306 (2012).
- [70] B. Nijboer and L. Van Hove, *Physical Review* **85**, 777 (1952).

Supplemental Material for: Universal Approach to Critical Percolation

Fabian Coupette^{1,*} and Tanja Schilling^{1,†}

¹*Institute of Physics, University of Freiburg, Hermann-Herder-Straße 3, 79104 Freiburg, Germany*

(Dated: September 1, 2023)

We briefly outline the central elements of connectedness percolation theory and illustrate that the corresponding low-order virial approximations are inconclusive.

I. VIRIAL EXPANSION FOR PERCOLATION

Connectedness percolation theory employs the cluster integral representation of the pair-correlation function in liquid state theory and adds the information of connectedness microscopically by modifying the Mayer f bond. The pair-connectedness is the analogue of the pair-distribution function in that the expression

$$P(\mathbf{r}, \mathbf{r}') d\mathbf{r} d\mathbf{r}' \quad (\text{S1})$$

describes the probability to simultaneously find particles in respective volume elements $d\mathbf{r}$ and $d\mathbf{r}'$ which are also part of the same connected component. Accordingly, the mean cluster size is given by

$$S(\mathbf{r}) = 1 + \int d\mathbf{r}' \rho(\mathbf{r}') P(\mathbf{r}, \mathbf{r}'), \quad (\text{S2})$$

which simplifies for a homogeneous system to

$$S = 1 + 4\pi\rho \int d\mathbf{r} r^2 P(r) = 1 + \rho \hat{P}(\mathbf{0}), \quad (\text{S3})$$

with $r = |\mathbf{r}' - \mathbf{r}|$ and $\hat{P}(\mathbf{k})$ denoting the Fourier transform of $P(\mathbf{r})$. The connectedness Ornstein-Zernike equation relates the pair connectedness P to the direct connectedness C^\dagger

$$P(\mathbf{r}_a, \mathbf{r}_b) = C^\dagger(\mathbf{r}, \mathbf{r}') + \int d\mathbf{r}'' C^\dagger(\mathbf{r}, \mathbf{r}'') \rho^{(1)}(\mathbf{r}'') P(\mathbf{r}'', \mathbf{r}'). \quad (\text{S4})$$

For a homogeneous system eq. (S4) is reduced to convolution which results in an algebraic equation in Fourier space

$$\hat{P} = \hat{C}^\dagger + \rho \hat{C}^\dagger \hat{P}. \quad (\text{S5})$$

This equation implies

$$\hat{P}(\mathbf{0}) = \frac{\hat{C}^\dagger(\mathbf{0})}{1 - \rho \hat{C}^\dagger(\mathbf{0})}, \quad (\text{S6})$$

so that, referring to eq. (S3), the mean cluster size diverges if the right hand side of eq. (S6) becomes singular. Assuming $C^\dagger(\mathbf{0})$ is finite, the smallest positive real root of

$$1 - \rho C^\dagger(\mathbf{0}) = 0 \quad (\text{S7})$$

corresponds to the percolation threshold. The virial expansion of C^\dagger in $f^\dagger(\mathbf{r}, \mathbf{r}') = \Theta(d - |\mathbf{r} - \mathbf{r}'|)$ bonds and ρ circles up to fourth virial order is given by

$$C^\dagger(\mathbf{r}, \mathbf{r}') = \begin{array}{cccc} \textcircled{r} \text{---} \textcircled{r'} & - 1 \text{ } \triangle & - 1 \text{ } \square & - 1 \text{ } \text{X} & + 1 \text{ } \text{Y} \\ + 1 \text{ } \text{Z} & + 1 \text{ } \text{W} & + 2 \text{ } \text{V} & - 2 \text{ } \text{U} & + \mathcal{O}(\rho^3) \end{array}, \quad (\text{S8})$$

* fabian.coupette@physik.uni-freiburg.de

† tanja.schilling@physik.uni-freiburg.de

The constituent diagrams have been calculated previously for the virial expansion of the structure of a hard sphere fluid for which the Mayer f bond is given by $f_{\text{HS}} \equiv -f^\dagger$. Yet, as commonly only the complete virial coefficients are reported, we list the analytic forms of the required integrals in table S1. The corresponding results for the left hand side of eq. (S7) are illustrated in Fig. S1. The third virial approximation does not yield a real root and hence does not predict a percolation threshold at all. The large discrepancy between all orders for rescaled densities exceeding $\rho d^3 \approx 0.2$ underline that higher order terms have substantial impact and the series cannot be reliably truncated at fourth (and presumably not even at much higher) orders. The Padé approximation does not resolve the issue that we have not included any of the important diagrams at densities close to the actual percolation threshold $\rho_c d^3 \approx 0.6530$.

Table S1. $C_i^\dagger(\mathbf{0})$ resulting from the individual diagrams of eq. S8 in the same order. The last expression utilizes a result from [S1].

virial order	diagram index	$C^\dagger(\mathbf{0})$
2	I	$\frac{4}{3}\pi d^3$
3	II	$\frac{5}{6}\pi^2 \rho d^6$
4	III	$\frac{2176}{2835}\pi^3 \rho^2 d^9$
4	(IV - VII)	$\frac{2357}{11340}\pi^3 \rho^2 d^9$
4	V & VI	$\frac{6347}{11340}\pi^3 \rho^2 d^9$
4	(IX - VIII)	$\frac{\pi^2 \rho^2 d^9}{22680} \left[4903\pi + 18(292\sqrt{2} - 3126 \operatorname{arccot}(\sqrt{2}) + 681 \operatorname{arccsc}(3) + 1248 \operatorname{arctan}(\frac{5}{\sqrt{2}})) \right]$

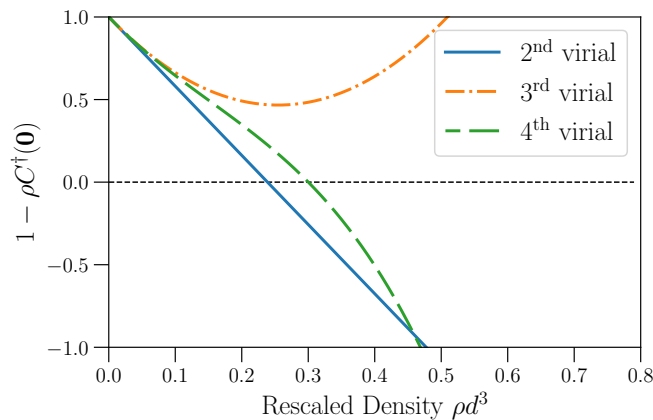


Figure S1. Virial approximations for percolation of fully penetrable spheres.

[S1] B. Nijboer and L. Van Hove, Radial distribution function of a gas of hard spheres and the superposition approximation, *Physical Review* **85**, 777 (1952).